Electronic Supplementary Information

Palladium Nanoparticles Stabilized by N-doped Porous Carbons Derived from Metal-Organic Frameworks for Selective Catalysis in Biofuel Upgrade: The Role of Catalyst Wettability

Yu-Zhen Chen,[a] Guorui Cai,[a] Yanmei Wang,[b] Qiang Xu,[c] Shu-Hong Yu,[a] and Hai-Long Jiang*[a]

[a]*Hefei National Laboratory for Physical Sciences at the Microscale, Key Laboratory of Soft Matter Chemistry, Chinese Academy of Sciences, Collaborative Innovation Center of Suzhou Nano Science and Technology, Department of Chemistry, University of Science and Technology of China, Hefei, Anhui 230026, P. R. China*

[b]*Department of Polymer Science and Engineering, University of Science and Technology of China, Hefei, Anhui 230026, P. R. China*

[c]*National Institute of Advanced Industrial Science and Technology (AIST), Ikeda, Osaka 563-8577, Japan*

*To whom correspondence should be addressed.

E-mail: jianglab@ustc.edu.cn

S1. Materials and Characterization

All chemicals were from commercial and used without further purification: palladium(II) nitrate aqueous solution ($Pd(NO_3)_2$, Shaanxi Kaida Chemical Engineering Co., Ltd., >5% Pd basis), Commercial 10% Pd/C (Shaanxi Kaida Chemical Engineering Co., Ltd). Etanol (>99%), hexahydrate ($Co(NO_3)_2 \cdot 6H_2O$, 99%, Sigma-Aldrich), N,N-dimethylformamide ($HCON(CH_3)_2$), methanol (>99%), benzoic acid (AR), acetone (AR), methanol (AR), tetrahydrofuran (THF, AR), KOH (AR), HCl (AR) and chloroform ($CHCl_3$) (AR) were purchased from Sinopharm Chemical Reagent Co., Ltd. $ZrCl_4$ (98%), zinc nitrate hexahydrate (99%), 2-methylimidazole (99%), zinc acetate dihydrate ($Zn(OAc)_2 \cdot 2H_2O$, 99%), sodium borohydride ($NaBH_4$, 98%), 2-methoxy-4-methyl-phenol (98%) and pyrrole (99%) were purchased from Energy Chemical (Shanghai, China). Triethylamine (99.0%), propionic acid (>99.5%), 4-hydroxymethyl-2-methoxy-phenol (98%) and 4-hydroxy-3-methoxy-benzaldehyde (vanillin, 99%) were purchased from Aladdin Industrial Inc. Terephthalic acid (>99.0%) was purchased from TCI. Distilled water with the specific resistance of 18.25 MΩ·cm was obtained by reversed osmosis followed by ion-exchange and filtration (Cleaned Water Treatment Co., Ltd., Hefei). Power X-ray diffraction (PXRD) were carried out on a Japan Rigaku DMax-γA rotation anode X-ray diffractometer equipped with graphite monochromatized Cu Kα radiation (λ = 1.54 Å). The contents of nitrogen, carbon and hydrogen were measured by using a VarioELIII Elemental analyzer. The content of Pd in the catalysts was quantified by an Optima

7300 DV inductively coupled plasma atomic emission spectrometer (ICP-AES). Field-emission scanning electron microscopy (FE-SEM) was carried out with a field emission scanning electron microanalyzer (Zeiss Supra 40 scanning electron microscope at an acceleration voltage of 5 kV). The transmission electron microscopy (TEM) and elemental mapping were acquired on JEOL-2010 and JEOL-2100F with an electron acceleration energy of 200 kV. Raman scattering spectra were recorded with a Renishaw System 2000 spectrometer using the 514.5 nm line of Ar^+ for excitation. X-ray photoelectron spectroscopy (XPS) measurements were performed by using an ESCALAB 250 high-performance electron spectrometer using monochromatized AlKa (hν = 1486.7 eV) as the excitation source. The static water contact angles (WCAs) were measured at room temperature using an Optical Contact Angle & Interface Tension Meter SL200KS (KINO, USA) equipped with CAST V2.28 software. Once a drop of water was deposited on tested surfaces and the contact angle determined from pictures were immediately captured. At least three measurements were made on each sample to obtain the values of contact angle. Nitrogen sorption measurement was conducted using a Micromeritics ASAP 2020 system at 77 K. Catalytic reaction products were analyzed and identified by gas chromatography (GC, Shimadzu 2010 Plus with a 0.25 mm × 30 m Rtx®-5 capillary column).

S2. Experimental Section.

Preparation of ZIF-8 nanocrystals: The synthesis of ZIF-8 nanocrystals is based on a previous procedure with some modifications.[1] Typically, 1.68 g of $Zn(NO_3)_2 \cdot 6H_2O$ was dissolved in 80 mL of methanol. A mixture of 3.70 g of 2-methylimidazole with 80 mL methanol was added to the above solution with vigorous stirring for 24 h at room temperature. The product was separated by centrifugation and washed thoroughly with methanol for twice, and finally dried overnight at 120 ^oC under vacuum condition.

Preparation of MOF-5: The synthesis of MOF-5 is based on a previous procedure with some modifications.[2] Typically, 0.507 g of terephthalic acid and 0.85 mL of triethylamine were dissolved in 40 mL of DMF. 1.7 g of $Zn(OAc)_2 \cdot 2H_2O$ was dissolved in 50 mL of DMF. The Zn-based solution was added to the ligand solution with stirring over 15 min, forming a precipitate, and the mixture was stirred for over 2.5 h. The precipitate was separated by centrifugation and immersed in DMF, evacuated at room temperature for over 12 h. It was then separated again and immersed in $CHCl_3$. The solvent was exchanged 2 times. The resultant MOF-5 powder was dried overnight at 120 ^oC under vacuum condition.

Preparation of ZIF-67: The synthesis of ZIF-67 is based on a previous procedure.[3] Typically, 0.45 g of cobalt nitrate hexahydrate was dissolved in 3 mL of deionized (DI) water; then 5.5 g of 2-methylimidazole (2-mim) in 20 mL of water was added into above solution under vigorously stirred for 6 h at room temperature. The resulting

purple precipitates were collected by centrifuging, washed with water and methanol in sequence for at least three times, and finally dried under vacuum at 50 ^{o}C overnight. The ZIF-67 powder was further activated at 150 ^{o}C under vacuum for 24 h prior to use.

Preparation of porous carbon materials.

NPC-ZIF-8-T: The 500 mg activated ZIF-8 powder was carbonized at different temperatures (600, 700, 800, 900 or 1000 ^{o}C) for 2 h at a heating rate of 5 ^{o}C min^{-1} in N_2 atmosphere. For the samples obtained at 600-800 ^{o}C, the residual Zn or/and ZnO species were removed by immersing in HCl aquous solution and washed by water.

NPC-ZIF-67: The 500 mg activated ZIF-67 powder was carbonized at 900 ^{o}C for 2 h at a heating rate of 5 ^{o}C min^{-1} in N_2 atmosphere. Next, the residual Co-based impurities were removed by immersing in HF aqueous solution (34 wt%) and washed by water.

C-MOF-5: The 500 mg activated MOF-5 powder was carbonized at 900 ^{o}C for 2 h at a heating rate of 5 ^{o}C min^{-1} in N_2 atmosphere.

Introducion of nitrogen into porous carbon and commercial activated carbon via urea treatment.

The additional nitrogen doping was realized by a hydrothermal reaction with 100 mg of original carbon materials (NPC-ZIF-8, C-MOF-5, NPC-ZIF-67 and AC) in 40.0 mL of 5.0 M urea aqueous solution at 180 ^{o}C for 12 h. During the process, the urea aqueous solution can easily permeate through the pores of the original carbon

materials. The products were washed thoroughly with water for at least three times, and finally dried overnight at 50 ^{o}C under vacuum.

Preparation of Pd NPs stabilized by MOF-derived porous carbons.

The Pd/MOF-derived porous carbon catalysts were prepared via an incipient-wetness impregnation method. Appropriate volume of 0.04 M H_2PdCl_4 aqueous solution was slowly added to the MOF-derived porous carbon. The mixture was allowed to stir at room temperature for 0.5 h and then dried at 50 ^{o}C for 12 h under vacuum. Finally, the sample was reduced at 200 ^{o}C for 4 h with 20% H_2/Ar in a flow rate of 40 mL/min.

S3. Evaluation of the Catalytic Performance of diverse carbon stabilized Pd NPs for biofuel upgrade.

The catalytic reaction was performed in a 10 mL Teflon-lined stainless steel autoclave equipped with a pressure gauge and a magnetic stirrer. The 50 mg of catalyst or 5 mg of commercial 10% Pt/C was dispersed in 3 mL of aqueous solution containing 89 mg of vanillin and the mixture was sonicated for about 20 min. The vessel was purged with H_2 for ten times, and then pressurized with H_2 to 0.2 MPa for reaction at desired temperatures. After reaction, the reactant and product were extracted by ethyl acetate and the rest aqueous solution was reused for the subsequent run by adding fresh vanillin directly under identical reaction conditions. The yield of the product was analyzed by GC.

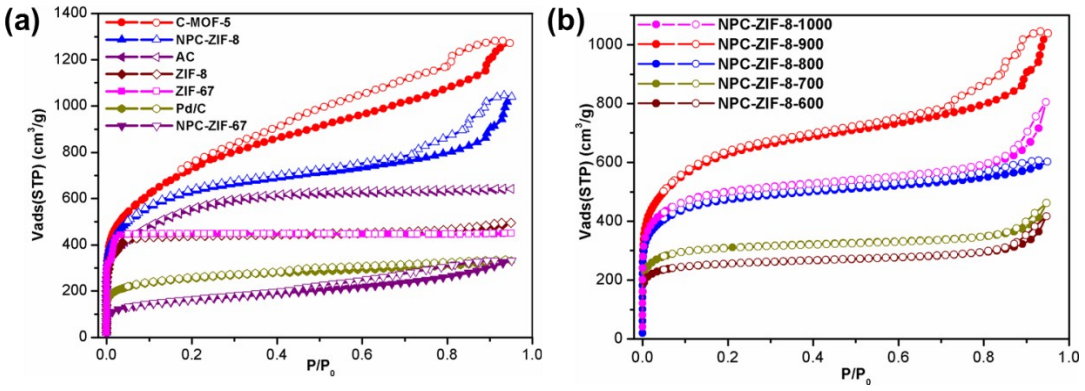

Fig. S1 N_2 sorption isotherms of (a) as-synthesized ZIF-67, ZIF-8, NPC-ZIF-8 (900 °C-2h), C-MOF-5 (900 °C-1h), NPC-ZIF-67 and commercial AC, Pd/C at 77 K, with corresponding BET surface areas of 1782, 1718, 2184, 2243, 573, 1856, 925 m^2/g, respectively. (b) NPC-ZIF-8 obtained at various pyrolysis temperatures, NPC-ZIF-8-1000, NPC-ZIF-8-800, NPC-ZIF-8-700, NPC-ZIF-8-600, give corresponding BET surface areas of 1856, 1726, 951, 784 m^2/g, respectively.

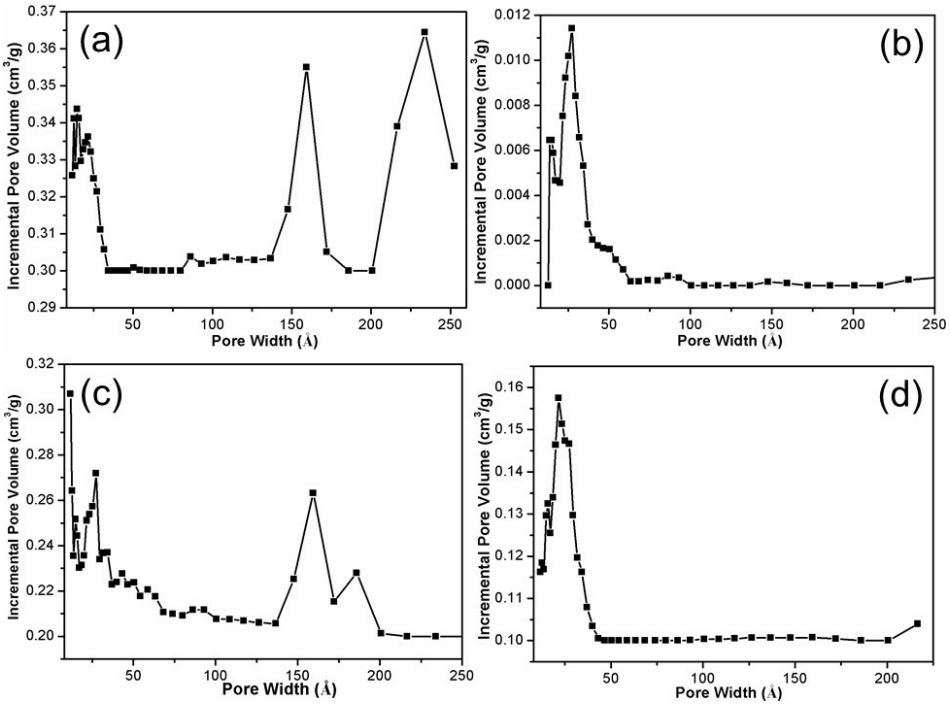

Fig. S2 Pore size distribution analyses for the several highly porous carbon materials (a) NPC-ZIF-8, (b) NPC-ZIF-67, (c) C-MOF-5 and (d) AC based on the density functional theory (DFT) method.

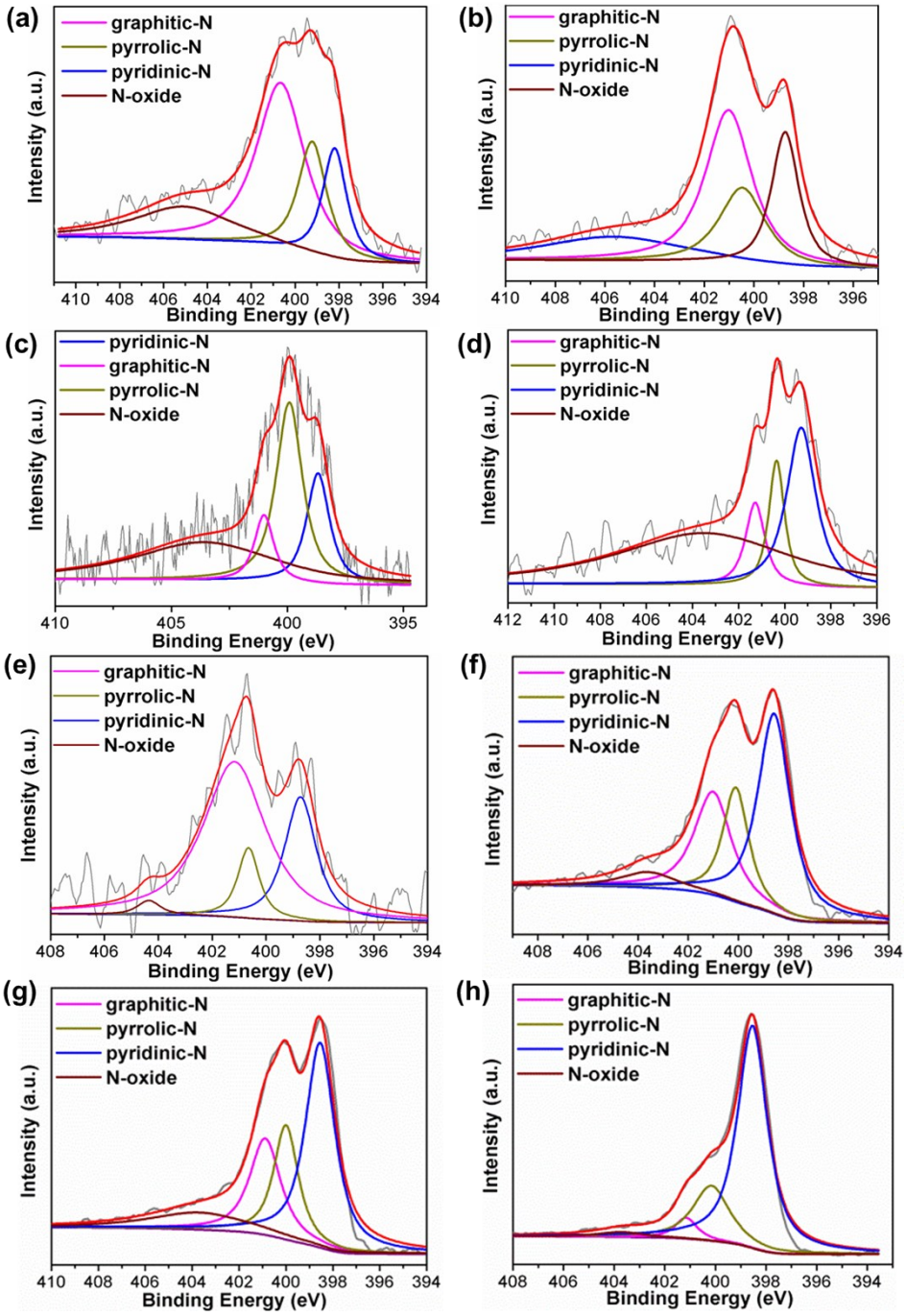

Fig. S3 XPS spectra of N 1s for N-doped carbon materials: (a) NPC-ZIF-8-urea, (b) NPC-ZIF-67, (c) C-MOF-5-urea, (d) AC-urea, (e) NPC-ZIF-8-900, (f) NPC-ZIF-8-800, (g) NPC-ZIF-8-700, and (h) NPC-ZIF-8-600.

Table S1. Surface concentration of N (at.%) and the N 1s analysis of XPS spectra for different samples.

Support	Graphitic-N (%)		Pyrrolic-N (%)		Pyridinic-N (%)		Oxide-N (%)	
	BE (eV)	at (%)	BE (eV)	at (%)	BE (eV)	at (%)	BE (eV)	at (%)
NPC-ZIF-8(-900)	401.12	68	400.68	4	398.74	26	404.47	2
NPC-ZIF-8-urea	400.7	46	399.21	19	398.19	16	405.03	19
C-MOF-5-urea	401.0	9	399.92	34	398.68	18	403.57	39
NPC-ZIF-67	400.96	49	399.4	26	398.58	25	-	0
AC-urea	401.27	9.3	400.3	11.4	399.28	27	403.48	52
NPC-ZIF-8-800	401.01	26	400.24	20	398.55	44	403.58	10
NPC-ZIF-8-700	400.87	22	399.99	21	398.54	45	403.69	12
NPC-ZIF-8-600	401.15	5	400.15	21	398.54	71	403.72	3

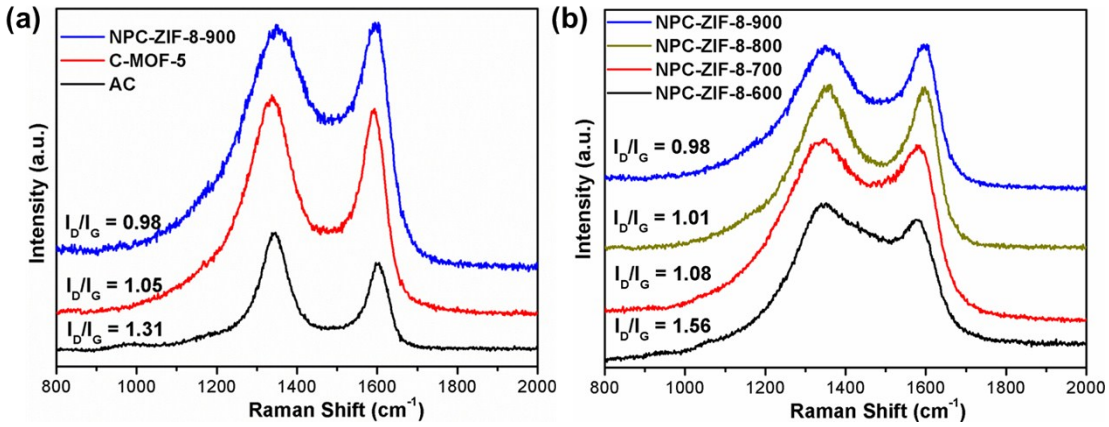

Fig. S4 Raman spectra for (a) NPC-ZIF-8, C-MOF-5 and AC, and (b) NPC-ZIF-8 obtained at various calcination temperatures. There are two dominant peaks at 1350 and 1600 cm^{-1}, corresponding to D and G bands, respectively. Notably, the I_D/I_G value of NPC-ZIF-8-900 (I_D/I_G = 0.98) is low in comparison with C-MOF-5 (I_D/I_G = 1.05) and AC (I_D/I_G = 1.35), indicating the highest degree of graphitization of the NPC-ZIF-8-900. Compared with AC, the wide D band for NPC-ZIF-8-900 and C-MOF-5 reveals the formation of abundant defects in disordered carbon during the heat-treated process. Fig. S4b shows that the higher degree of graphitization of NPC-ZIF-8 can be obtained with increasing pyrolysis temperatures.

Table S2. Element analysis results for the several porous carbon materials.

Support	N (wt%)	C (wt%)	H (wt%)
NPC-ZIF-8-900	2.39	83.07	1.56
NPC-ZIF-8-urea	2.94	78.99	2.53
C-MOF-5	0.51	83.37	1.86
C-MOF-5-urea	3.42	79.25	2.47
NPC-ZIF-67	2.26	83.07	1.02
AC-urea	1.31	91.12	1.34
NPC-ZIF-8-800	5.09	69.76	2.82
NPC-ZIF-8-700	13.72	55.75	3.17
NPC-ZIF-8-600	18.61	55.21	4.57

Table S3. Inductively coupled plasma atomic emission spectrometry (ICP-AES) analysis for Pd content in all catalysts.

Catalysts	Pd content (%)
Pd/NPC-ZIF-8	0.62
Pd/NPC-ZIF-8-urea	0.6
Pd/NPC-ZIF-67	0.88
Pd/C-MOF-5	0.89
Pd/MOF-5-urea	1.1
Pd/AC	0.69
Pd/AC-urea	0.6
Pd/Al_2O_3	0.78
Pd/TiO_2	0.54
Pd/SiO_2	0.84

The inconsistency of Pd contents among different Pd-based catalysts may be caused by: 1) the different sources of Pd precursor in the catalyst synthesis. Some of $Pd(NO_3)_2$ precursor was prepared from $PdCl_2$ while the other $Pd(NO_3)_2$ precursor was commercial, which would bring about the deviation of Pd content; 2) the experimental error during the sample weighing (both preparing the supported catalysts and also ICP measurement), as the carbons are highly porous and they are prone to absorb water during handling in air.

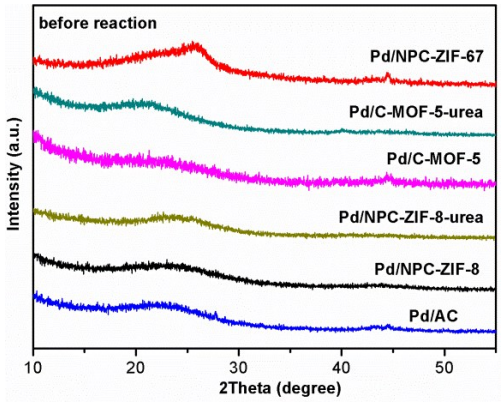

(a)

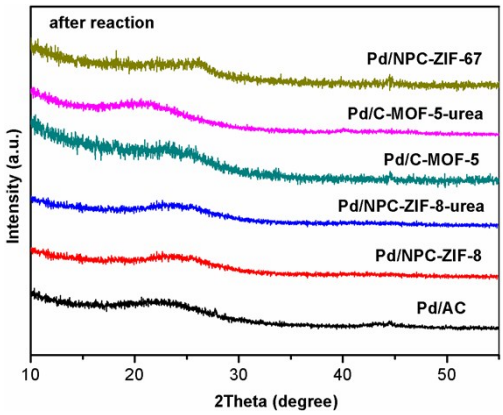

(b)

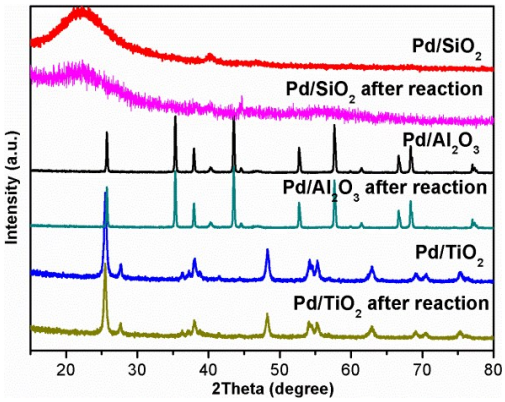

(c)

Fig. S5 Powder XRD patterns for Pd NPs stabilized by MOF-derived carbon materials and commercial AC catalysts (a) before reaction and (b) after reaction. (c) Powder XRD patterns for commercial inorganic oxides (SiO_2, TiO_2 and Al_2O_3) supported Pd NPs before and after catalytic reaction.

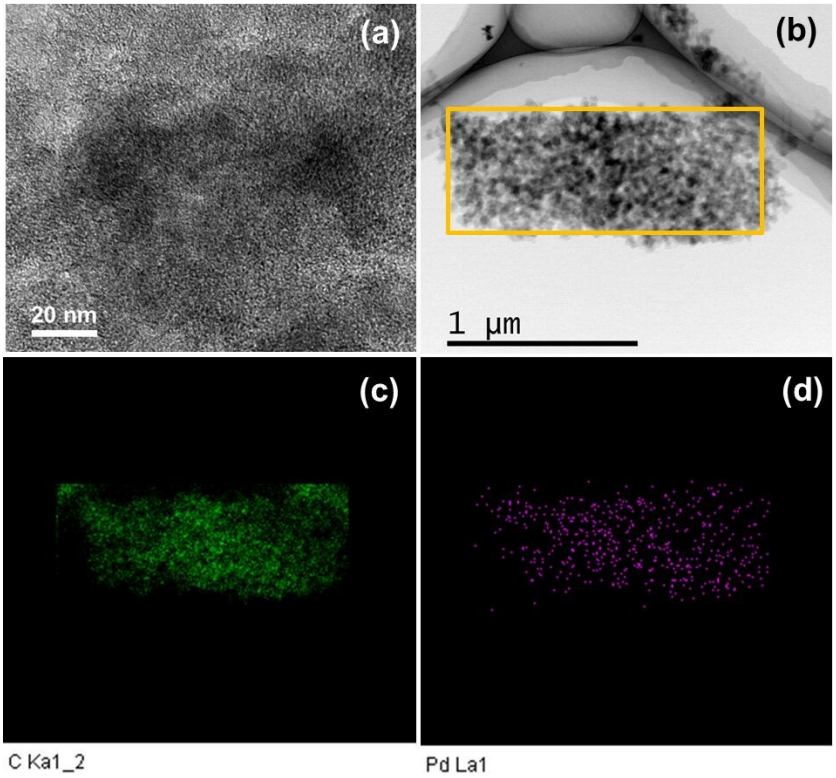

Fig. S6 (a,b) TEM images and the corresponding (c) C and (d) Pd element mappings for as-synthesized Pd/NPC-ZIF-8 catalyst, showing the uniform distribution of ultrafine Pd NPs throughout the porous carbon.

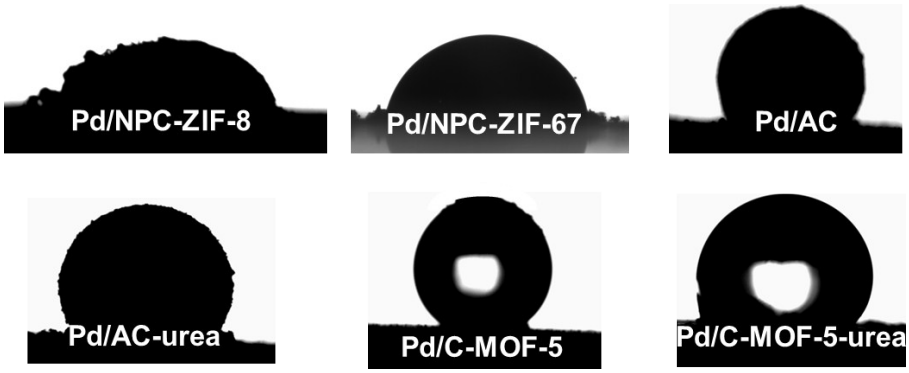

Fig. S7 The air-water contact angles for Pd/NPC-ZIF-8, Pd/NPC-ZIF-67, Pd/AC，Pd/AC-urea, Pd/C-MOF-5 and Pd/C-MOF-5-urea catalysts. The samples have the similar contact angles to the corresponding parent MOF-derived porous carbons, indicating that the wettability of MOF-derived porous carbons is well retained upon loading Pd NPs.

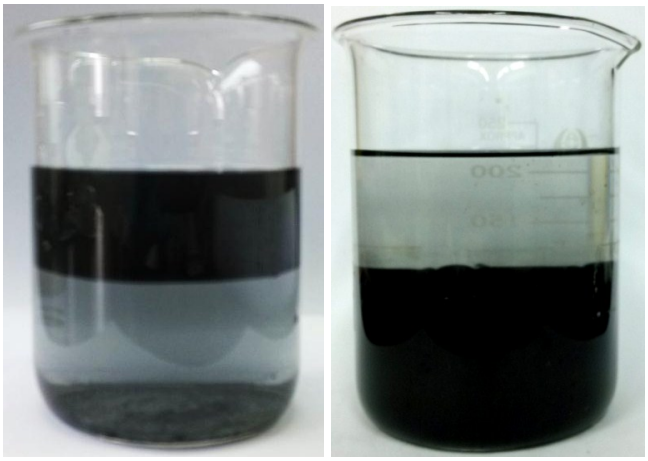

Pd/AC **Pd/NPC-ZIF-8**

Fig. S8 The Pd/AC and Pd/NPC-ZIF-8 catalysts with different wettability are dispersed in the upper organic solution (ethyl acetate) and the bottom aqueous solution (water), respectively.

Table S4. Catalytic results for HDO of vanillin at different temperatures in aqueous solution.[a]

Reaction temperature (°C)	Time (h)	Conversion[b] (%)	Selectivity[b] (%)	
			B	A
70	12	99	5	95
90	2	100	0	100
110	1.5	99	2	98

[a]Reaction conditions: vanillin (89 mg, 0.585 mmol), 0.6% Pd/NPC-ZIF-8 (50 mg), water (3 mL), H_2 (0.2 MPa) at different temperatures. [b]Conversion and selectivity were analyzed by GC.

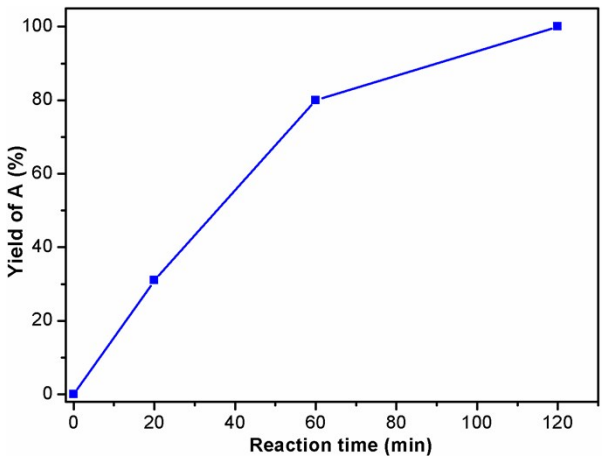

Fig. S9 The concentration evolution of target product **A** along with reaction time in the experiment performed with vanillin over Pd/NPC-ZIF-8. Reaction conditions: vanillin (89 mg, 0.585 mmol), Pd/NPC-ZIF-8 (50 mg), S/C (molar ratio of substrate/metal) = 208, water (3 mL), H_2 (0.2 MPa), 90 ^{o}C.

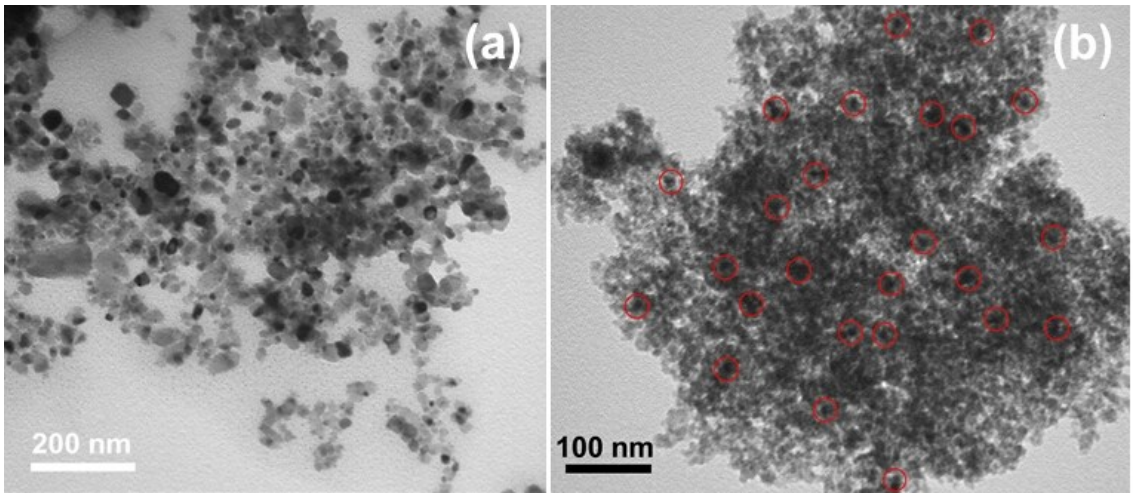

Fig. S10 TEM images of (a) Pd/TiO_2 and (b) $Pd/\gamma\text{-}Al_2O_3$.

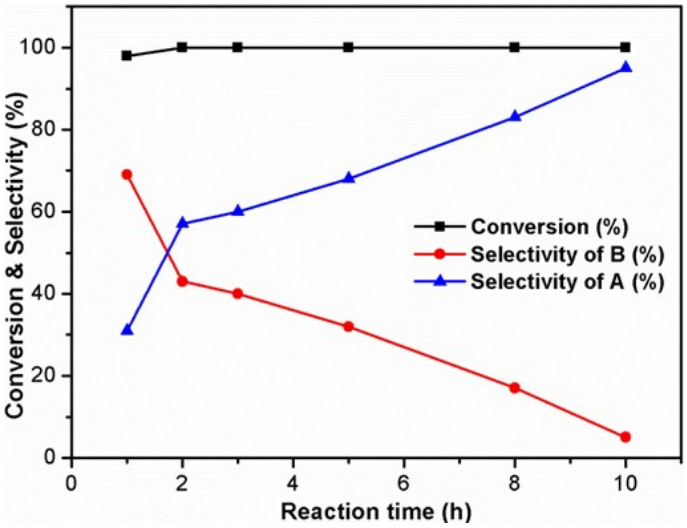

Fig. S11 Catalytic results for HDO of vanillin at 0.1 MPa H_2 in aqueous solution. Reaction conditions: vanillin (89 mg, 0.585 mmol), 0.6% Pd/NPC-ZIF-8 (50 mg), water (3 mL), 90 ^oC, H_2 bubbling.

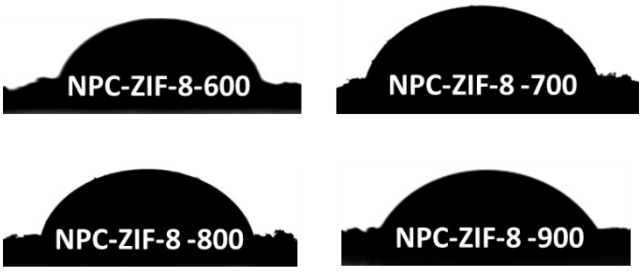

Fig. S12 The air-water contact angles for NPC-ZIF-8 with different pyrolysis temperatures. All these samples present similar contact angles.

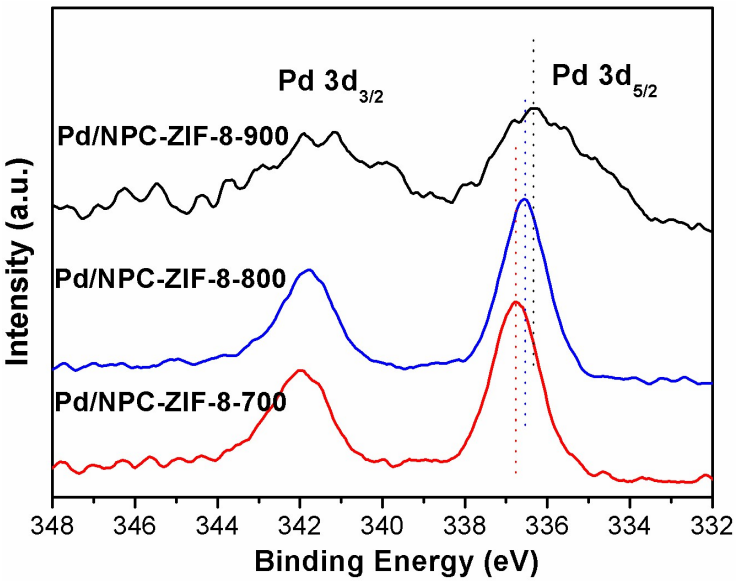

Fig. S13 XPS spectra of Pd 3d for Pd/NPC-ZIF-8-900, Pd/NPC-ZIF-8-800 and Pd/NPC-ZIF-8-700.

Table S5. Catalytic performance comparison for Pd/NPC-ZIF-8 and reported catalysts.

Catalyst	Reaction temperature (^{o}C)	Reaction time (h)	Reaction pressure (MPa)	TOF (h^{-1})[a]	Ref
Pd/NPC-ZIF-8	90	1	0.2	160	This work
Pd/NPC-ZIF-8	90	10	0.1	19	This work
$Pd/CN_{0.132}$	90	15	0.1	1.66	4
Pd/CM170	100	1	1	52	5
Pd/MSMF	110	2	1	225	6
Au/CNT	150	8	1	17.3	7
Pd@MIL-101	100	2	0.2	14.3	8

[a]Calculated based on the target product.

References

1 S. R. Venna, J. B. Jasinski, and M. A. Carreon, *J. Am. Chem. Soc.*, 2010, **132**, 18030-18033.

2 D. J. Tranchemontagne, J. R. Hunt and O. M. Yaghi, *Tetrahedron*, 2008, **64**, 8553-8557.

3 J. Qian, F. Sun, and L. Qin, *Mater. Lett.*, 2012, **82**, 220-223.

4 X. Xu, Y. Li, Y. Gong, P. Zhang, H. Li and Y. Wang, *J. Am. Chem. Soc.*, 2012, **134**, 16987-16990.

5 Z. Zhu, H. Tan, J. Wang, S. Yu and K. Zhou, *Green Chem.*, 2014, **16**, 2636-2643.

6 Z. Lv, Q. Sun, X. Meng and F.-S. Xiao, *J. Mater. Chem. A*, 2013, **1**, 8630-8635.

7 X. Yang, Y. Liang, X. Zhao, Y. Song, L. Hu, X. Wang, Z. Wang and J. Qiu, *RSC Adv.*, 2014, **4**, 31932-31936.

8 A. Aijaz, Q.-L. Zhu, N. Tsumori, T. Akita and Q. Xu, *Chem. Commun.*, 2015, **51**, 2577-2580.